Anesthesia with Dexmedetomidine and Low-dose Isoflurane Increases Solute Transport *via* the Glymphatic Pathway in Rat Brain When Compared with High-dose Isoflurane

Helene Benveniste, M.D., Ph.D., Hedok Lee, Ph.D., Fengfei Ding, M.D., Ph.D., Qian Sun, Ph.D., Ehab Al-Bizri, M.D., Rany Makaryus, M.D., Stephen Probst, M.D., Maiken Nedergaard, M.D., Ph.D., Elliot A. Stein, Ph.D., Hanbing Lu, Ph.D.

ABSTRACT

Background: The glymphatic pathway transports cerebrospinal fluid through the brain, thereby facilitating waste removal. A unique aspect of this pathway is that its function depends on the state of consciousness of the brain and is associated with norepinephrine activity. A current view is that all anesthetics will increase glymphatic transport by inducing unconsciousness. This view implies that the effect of anesthetics on glymphatic transport should be independent of their mechanism of action, as long as they induce unconsciousness. We tested this hypothesis by comparing the supplementary effect of dexmedetomidine, which lowers norepinephrine, with isoflurane only, which does not.

Methods: Female rats were anesthetized with either isoflurane (N = 8) or dexmedetomidine plus low-dose isoflurane (N = 8). Physiologic parameters were recorded continuously. Glymphatic transport was quantified by contrast-enhanced magnetic resonance imaging. Cerebrospinal fluid and gray and white matter volumes were quantified from T1 maps, and blood vessel diameters were extracted from time-of-flight magnetic resonance angiograms. Electroencephalograms were recorded in separate groups of rats.

Results: Glymphatic transport was enhanced by 32% in rats anesthetized with dexmedetomidine plus low-dose isoflurane when compared with isoflurane. In the hippocampus, glymphatic clearance was sixfold more efficient during dexmedetomidine plus low-dose isoflurane anesthesia when compared with isoflurane. The respiratory and blood gas status was comparable in rats anesthetized with the two different anesthesia regimens. In the dexmedetomidine plus low-dose isoflurane rats, spindle oscillations (9 to 15 Hz) could be observed but not in isoflurane anesthetized rats.

Conclusions: We propose that anesthetics affect the glymphatic pathway transport not simply by inducing unconsciousness but also by additional mechanisms, one of which is the repression of norepinephrine release. **(Anesthesiology 2017; 127:976-88)**

THE glymphatic pathway is a newly discovered system that clears waste, including amyloid-β (Aβ),[1] tau,[2] and lactate[3] from the brain. Therefore, a plausible hypothesis has recently emerged, positing that malfunction of the glymphatic waste clearance system of the brain may contribute to the pathogenesis of Alzheimer disease (AD).[4] Anatomically, the glymphatic pathway is defined by the perivascular compartment of the cerebral vascular network.[1] The outer perimeter of the perivascular space is made up by glial endfeet characterized by high, polarized expression of aquaporin 4 water channels.[1] Studies suggest that the glymphatic pathway removes waste in the following manner: cerebrospinal fluid (CSF) is transported from the subarachnoid space into the brain *via* the periarterial spaces[1]; the aquaporin 4 water channels on the glial endfeet help boost transport of CSF from the perivascular compartment into the interstitial fluid (ISF) space.[1] The CSF-ISF exchange process facilitates interstitial waste removal *via* perivenous conduits and along cranial

What We Already Know about This Topic

- The glymphatic pathway is a process whereby waste materials are removed from the brain. Slow-wave sleep, suppression of noradrenergic signaling, and anesthesia-induced unconsciousness all increase glymphatic transport.
- It is not clear whether anesthetic-induced increase in transport is due to loss of consciousness *per se* or due to specific pharmacologic effects of anesthetic agents.
- Using state-of-the-art magnetic resonance imaging techniques, glymphatic transport during anesthesia produced by isoflurane alone was compared with dexmedetomidine in combination with low-dose isoflurane.

What This Article Tells Us That Is New

- Glymphatic transport was significantly greater in animals to whom dexmedetomidine and low-dose isoflurane were administered in comparison with isoflurane alone.
- These data suggest that specific pharmacologic effects, especially suppression of noradrenergic neurotransmission, are more relevant in the increase in glymphatic transport than anesthesia-induced unconsciousness, *per se*.

This article is featured in "This Month in Anesthesiology," page 1A. Supplemental Digital Content is available for this article. Direct URL citations appear in the printed text and are available in both the HTML and PDF versions of this article. Links to the digital files are provided in the HTML text of this article on the Journal's Web site (www.anesthesiology.org).

 Anesthesiology 2017; 127:976-88

<zdoi;10.1097/ALN.0000000000001888>

nerves[1,5,6] to ultimately drain *via* lymph vessels located in the meninges,[7] head, and the neck.[8] The polarized aquaporin 4 expression pattern on glial endfeet is essential for efficient waste clearance.[1] For example, in aging or traumatic brain injury, loss of aquaporin 4 polarization slows down clearance of Aβ and tau[9]; and in postmortem brain tissue from humans afflicted with AD, the aquaporin 4 expression pattern is inhomogeneous and associated with Aβ plaques.[10]

The main controllers of glymphatic waste clearance include intracranial pressure differentials,[11] cardiac pulsation,[12] and regulators of ISF space volume.[13] For example, changes in body posture impacts glymphatic transport and Aβ clearance from brain.[14] A most intriguing feature of glymphatic pathway function is its dependency on state of arousal,[13] such that glymphatic transport of solutes (including Aβ) accelerates during slow-wave sleep or general anesthesia when compared with wakefulness.[13] The underlying mechanism(s) responsible for reduced brain waste removal during wakefulness compared with sleep is not well understood but is associated with central norepinephrine activity, because central blockade with α-adrenergic blockers mimics the effect.[13] Given the association among brain waste removal, norepinephrine activity, and state of arousal,[3,15] a key question to address would be how anesthetics with different mechanisms of action but with common effects on the state of consciousness influence glymphatic transport patterns. This is important because there may be clinical benefit to enhancing the glymphatic transport of the brain during anesthesia or sedation procedures, which could be accomplished if drugs with central norepinephrine-lowering effects are used.

Dexmedetomidine is routinely administered to patients in intensive care units and anesthesia settings.[16] Dexmedetomidine is a selective α2 agonist that hyperpolarizes locus coeruleus neurons, decreasing their firing rate and norepinephrine release,[17] thereby inducing a hypnotic effect. Sedation with dexmedetomidine induces a state similar to stage II sleep with an increase in slow-wave activity (0.5 to 3.5 Hz).[18] In contrast, inhalational agents such as isoflurane induce hypnosis, analgesia, amnesia, and relaxation by interactions with γ-aminobutyric acid receptor type A, *N*-methyl-D-aspartate, and glycine receptors.[19] Isoflurane administered at 1.5 to 2.0 minimum alveolar concentration reduces locus coeruleus activity but paradoxically increases norepinephrine in the preoptic hypothalamus[20] and is associated with burst suppression. Given the diverse effects of dexmedetomidine and isoflurane on central norepinephrine, we tested the hypothesis that glymphatic transport would be more efficient during anesthesia that combines dexmedetomidine with low-dose isoflurane compared with isoflurane only in the rodent brain.

Submitted for publication February 27, 2017. Accepted for publication August 16, 2017. From the Department of Anesthesiology, Yale School of Medicine, New Haven, Connecticut (H.B., H.L.); Center for Translational Neuromedicine, University of Rochester, Rochester, New York (F.D., Q.S., M.N.); Department of Anesthesiology, Stony Brook Medicine, Stony Brook, New York (E.A.-B., R.M., S.P.); National Institute on Drug Abuse, Intramural Research Program, Baltimore, Maryland (E.A.S., H.L.).

To test this hypothesis we use our previously developed magnetic resonance (MR) imaging (MRI)–based platform for quantifying glymphatic transport in the rodent brain.[21]

Materials and Methods

Animals

The local institutional animal care and use committees at the National Institute on Drug Abuse Intramural Research Program (Baltimore, Maryland), Stony Brook University (Stony Brook, New York), Rochester University (Rochester, New York), and Yale University (New Haven, Connecticut) approved all of the animal work. To test our hypothesis, rats were divided into six experimental groups (table 1). Female Fisher 344 rats (200 to 300 g) were used in groups 1, 2, 5, and 6, and female Sprague Dawley rats were used in group 3 and 4 experiments (see Supplemental Digital Content, http://links.lww.com/ALN/B540). Groups 1 and 2 were used to directly test the hypothesis that brain-wide glymphatic transport of the small molecular weight paramagnetic contrast agent gadopentetic acid (Gd-DTPA; molecular weight = 938 Da) would be superior with dexmedetomidine plus low-dose isoflurane (DEXM-I) when compared with isoflurane anesthesia. Groups 3 and 4 tested the effects of the two anesthetics regimens on arterial blood gas values of the spontaneously breathing rats measured during MRI, which we assumed would be similar between groups. Finally, and outside the MRI, groups 5 and 6 were used to test the hypothesis that spindles would be present in the electroencephalogram of DEXM-I anesthetized rats compared with isoflurane, indicating different arousal patterns with the two drugs.

MRI Experiments (Groups 1 and 2)

All of the MRI acquisitions were performed on a 9.4-T/30 MR instrument interfaced to a Bruker Advance console controlled by Paravision 6.0 software (Bruker Bio Spin, USA). Rats were scanned in the supine position using a custom-built animal cradle system, and small earplugs with external gauze pads were accommodated onto the ears of the rats to minimize the noise from the scanner. A 2-cm planar surface radiofrequency coil (Bruker) with a built-in preamplifier was used as a receiver, and an 86-mm diameter volume coil (Bruker) was used as a transmitter.

Anesthesia and Surgery for Animals Undergoing MRI. Group 1 and 2 rats underwent implantation of an intrathecal catheter into the cisterna magna, as described previously.[14,21] After surgery, rats were prepared for MRI and the anesthesia regimen adjusted according to table 1. For group 1 rats, isoflurane anesthesia was maintained at 1.5 to 2.2% delivered in an 1:1 oxygen:air mixture *via* a nose cone. Exhaled gas from the rats was actively vacuumed away from the nose cone *via* a built-in vacuum line. For group 2 rats, 0.015 mg/kg of dexmedetomidine was administered intraperitoneally and followed by a continuous infusion of 0.015 to 0.020 $mg \cdot kg^{-1} \cdot h^{-1}$ delivered *via* a subcutaneous catheter. Low-dose isoflurane

Table 1. Experimental Groups and Experiments

Groups	Anesthesia	Experiment	MRI	Arterial Line	Electroencephalogram
1 (N = 8)	Isoflurane	Characterizing glymphatic transport of Gd-DTPA	Yes	No	No
2 (N = 8)	DEXM-I		Yes	No	No
3 (N = 4)*	Isoflurane	Characterizing physiologic parameters	Yes	Yes	No
4 (N = 4)*	DEXM-I		Yes	Yes	No
5 (N = 4)	Isoflurane	Characterizing electroencephalogram	No	No	Yes
6 (N = 4)	DEXM-I		No	No	Yes

*Female Sprague Dawley rats were used for the additional studies (see Supplemental Digital Content, http://links.lww.com/ALN/B540, for more information). DEXM-I = dexmedetomidine plus low-dose isoflurane; Gd-DTPA = gadopentetic acid.

(0.4 to 0.8% isoflurane) was used as supplementary anesthesia for group 2 rats to enhance motor relaxation during the MRI scanning procedure; this anesthesia routine is referred to as *DEXM-I* in the article. Physiologic parameters, including respiratory rate (RR), oxygen saturation, body temperature, and heart rate (HR), were continuously monitored using an MRI-compatible monitoring system (SA Instruments, USA). Body temperature was kept within a range of 36.5° to 37.5°C using a heated waterbed.

The MRI imaging experiments included the following: (1) precontrast T1 mapping for quantitative assessment of gray matter, white matter, and CSF; (2) glymphatic transport characterization using contrast enhanced MRI; and (3) MR angiography.

T1 Mapping. In a subset of animals in groups 1 and 2, variable flip angle spoiled gradient echo method was implemented to quantify corresponding three-dimensional (3D) longitudinal relaxation (T1) maps, which were used for volumetric tissue compartment analyses. After acquisition of scout images, 3D T1 mapping was performed with the following parameters: repetition time (TR)/echo time (TE) = 15/4 ms, scanning time = 4 min, dummy = 10, matrix = 128 × 128 × 128 reconstructed at 0.24 × 0.24 × 0.26 mm. A set of six flip angles (2°, 5°, 10°, 15°, 20°, and 30°) were acquired for T1 maps. The spatial inhomogeneity profile of the radiofrequency transmit was acquired using a double angle method[22] as a correction factor for the T1 mapping procedure. Rapid acquisition with relaxation enhancement sequence was implemented for B1 mapping of the radiofrequency transmit using the following parameters: TR = 10,000 ms, TE = 22 ms, average = 1, rapid acquisition with relaxation enhancement factor = 4, number of slices = 50, in plane resolution = 0.24 mm/pixel, slice thickness = 0.4 mm, slice gap = 0.2 mm, and flip angles = 70° and 140°.

Glymphatic Transport MRI. Spoiled gradient echo fast low angle shot (FLASH) 3D images were acquired (TR = 15 ms, TE = 4.1 ms, number of excitations [NEX] = 1) every 4 min. Images were interpolated from 256 × 128 × 128 to 256 × 256 × 256, yielding a nominal spatial resolution of 0.12 × 0.12 × 0.13 mm.^{3} The first three images were taken as baseline images, and Gd-DTPA contrast infusion was started at the beginning of the fourth image. A 1:40 dilution (Gd-DTPA:water) was infused at a rate of 1.7 μl/min for a total volume of 20 μl. FLASH 3D images were acquired continuously for at least 160 min, totaling approximately 40 frames for each study.

MR Angiogram. A two-dimensional (2D) time-of-flight MR angiogram sequence (TR = 12 ms, TE = 2.7 ms, NEX = 4, flip angle = 80°) was taken at the end of the study with a spatial image resolution of 0.12 × 0.12 × 0.20 mm^3 (256 × 256 × 105). Translation and orientation of the 2D MR angiograms were adjusted so that both MR angiogram and FLASH 3D images were spatially coregistered.

MRI Data Analysis

Calculation of 3D T1 Maps. The 3D T1 mapping was performed by linearization of the spoiled gradient echo signal in canonical form, which was then solved voxelwise by an unweighted linear least-square fit algorithm.[23] For calculating T1, the radiofrequency inhomogeneity correction factor was applied onto the flip angles to correct for nominal flip angles with actual flip angles.[24–26]

T1 Map Spatial Normalization and Tissue Segmentation. Individual T1 maps were segmented into gray matter, white matter, and CSF probability maps using a unified segmentation algorithm in SPM12 (http://www.fil.ion.ucl.ac.uk/spm; accessed August 2017)[27] using the *in vivo* rat tissue probability maps[28] as spatially resolved tissue priors. Segmented gray matter and white matter tissue probability maps in native space were then thresholded and summed for calculating total volumes in each compartment.

Analysis of Glymphatic Transport from Contrast-enhanced MRI Dynamic Images. Contrast-enhanced MRI images were processed as described previously.[14,21] Briefly, all of the images were exported in DICOM and converted into nifti file format to correct for head motion, intensity normalization across the time series, and spatial smoothing. After spatial smoothing, percentage of signal changes from the baseline were calculated in each voxel, as described previously.[14,21] From each of the parametric dynamic MRI images, time signal curves (TSCs) of Gd-DTPA–induced signal changes were extracted using PMOD software (version 3.5; PMOD Technologies Ltd., Switzerland) from regions of interest using the baseline MRI as an anatomic template. A whole-brain parenchymal mask was created for each of the rats' anatomic T1 templates by excluding CSF spaces and the TSCs extracted. TSCs from other regions

of interest were extracted from the dynamic T1-weighted images, including the hippocampus and olfactory tubercle. To calculate whole-brain Gd-DTPA uptake (representing glymphatic transport), the area under the curve of the TSCs (0 to 180 min) from the whole brain were extracted from the dynamic MRI images from each rat using PMOD software, as described previously.[21] From the hippocampal TSCs, time to peak, peak magnitude, and clearance rates were estimated by linearly fitting the descending trend.[29] Volumetric rendering of Gd-DTPA distributions at various time after CSF administration were enabled using Amira software (version 6.2; FEI, Thermo Fisher Scientific, USA).

Analysis of MR Angiograms. The MR angiograms were reformatted to match the spatial resolution of the 3D FLASH images acquired for visualizing Gd-DTPA glymphatic transport. The MR angiogram analysis was performed similar to that outlined by Li *et al.*[30] by implementing the autoskeleton pipeline in Amira software. The MR angiogram image was displayed using maximum intensity projection; to measure vessel lumen diameter, radial projections perpendicular to the vessel of interest were obtained and the mean diameter along the vessel segment calculated.

Measurement of Physiologic Parameters and Blood Gases (Groups 3 and 4)

In a separate series of rats (groups 3 and 4, Supplemental Digital Content, http://links.lww.com/ALN/B540), we measured physiologic parameters and blood gases receiving either isoflurane or DEXM-I similar to groups 1 and 2. Rats were initially anesthetized with isoflurane, an arterial catheter was inserted into the femoral artery, and cisterna magna catheter sham operation was performed. The skin wounds were closed. The rats were randomly assigned to receive either isoflurane or DEXM-I, and the anesthetic regimens and physiologic monitoring were carried out as for groups 1 and 2. The rats were placed in the 9.4-T instrument, and MRI scanning was started. Arterial blood gases were acquired twice over 1 h. The spinal catheter was not perfused with contrast for these experiments (for more details, see Supplemental Digital Content, http://links.lww.com/ALN/B540).

Electroencephalogram Measurements during Isoflurane and DEXM-I (Groups 5 and 6)

Electromyogram and electroencephalogram recording electrodes were prepared as described previously.[31] Briefly, six-channel, custom-made electroencephalogram/electromyogram recording electrodes were prepared by soldering small (less than 0.75-inch) segments of insulated 0.008-inch silver wire into gold-pin connectors. These electrodes were then combined into a six-channel electroencephalogram electrode holder and secured using dental cement. The electroencephalogram and electromyogram recording wires were inserted over the surface of the skull (four electrodes) and the neck musculature (two electrodes). For group 5 rats undergoing electroencephalogram recording inhaled with isoflurane, anesthesia was induced with 2 to 3% isoflurane in 100% O_2 until the righting reflex was lost and maintained with 1.5 to 1.8% isoflurane delivered in 1:1 oxygen:air mixture *via* a nose cone. The RR was maintained between 55 to 65 breaths/min by adjusting the isoflurane concentration. For group 6, rats were first induced with 2 to 3% isoflurane in 100% O_2 until loss of the righting reflex; subsequently, a 0.015 mg/kg bolus of dexmedetomidine was administered intraperitonally (repeated two to four times if RR was more than 40 breaths/min) followed by a continuous infusion of (0.015 to 0.020 mg $\cdot$ kg^{-1} $\cdot$ h^{-1}) delivered *via* a subcutaneous catheter placed in the flank area. Low-dose isoflurane (0.4 to 0.8% isoflurane) was used as supplementary anesthesia. The RR was maintained at approximately 40 breaths/min by adjusting the isoflurane concentration. RR and temperature were monitored every 10 min for 1.5 to 2.0 h. Body temperature was kept within a range of 36.5° to 37.5°C using a heating pad. The rats were in prone position during anesthesia and electroencephalogram recordings. Electroencephalogram recordings were collected using an XLTEK 32-channel electroencephalogram system. Electrodes were referenced to one skull electrode and saved using XLTEK; data were analyzed using customized Matlab scripts to determine percentage of prevalence (delta: 1 to 4 Hz, theta: 4 to 8 Hz, alpha: 8 to 13 Hz, β: 13 to 32 Hz) and power spectrum.

Statistical Analyses

All of the statistical analyses was performed using XLSTAT software (version 2016.5, Addinsoft, France). Sample size for MRI-based glymphatic studies (groups 1 and 2) was based on previous experience.[14,21] Whole-brain Gd-DTPA uptake as measured by area under the curve of the TSCs for more than 180 min (AUC_{180}) were compared between the two groups using a two-tailed *t* test for independent groups, and a *P* value less than 0.05 was considered significant. All of the continuous variables, including HR, RR, and mean blood pressure (see Supplemental Digital Content, http://links.lww.com/ALN/B540), were tested to determine whether they met conditions of normality using the Shapiro–Wilk test. The differential effects of the two anesthesia regimens on HR and RR were analyzed by first calculating the mean of these parameters for each rat for more than 180 min. Subsequently, the coefficients of variation of the HR and RR were calculated for each rat over the 180 min of experimental recording. Mann–Whitney, two-tailed test was used to compare the mean HR, RR, and mean coefficients of variation among the groups. The vessel analyses performed from the MR angiograms were performed blindly. To evaluate group differences (DEXM-I *vs.* isoflurane) between parameters including parameters extracted from the hippocampal TSC (time to peak, peak magnitude, and clearance rates), vessel diameter, tissue compartments (CSF, white matter, and gray matter), and blood gas values, the Student *t* test was used if normality was met, and the Mann–Whitney, two-tailed test was performed if normality was unmet. All of the data are presented as mean ± SD.

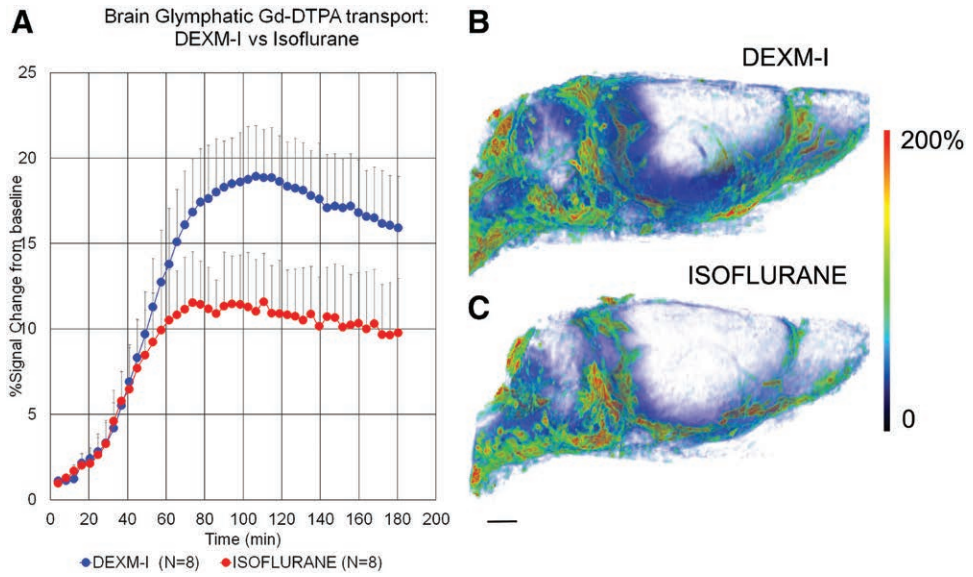

Fig. 1. Dexmedetomidine and low-dose isoflurane (DEXM-I) enhances glymphatic transport of gadopentetic acid (Gd-DTPA) in comparison with isoflurane. (*A*) Average time signal curves (TSC) of Gd-DTPA–induced signal changes from whole brain of rats anesthetized with DEXM-I (*blue, filled circles*) and isoflurane (*red, filled circles*). The TSCs were extracted from the dynamic contrast-enhanced T1-weighted magnetic resonance images (MRIs) and represent glymphatic transport of brain parenchyma (excluding cerebrospinal fluid compartment). There is overall more whole-brain uptake (as measured by percentage of signal change from baseline) of Gd-DTPA in the DEXM-I–anesthetized rats when compared with isoflurane (see Results section for quantitative details). The data are expressed as mean ± SD. (*B* and *C*) Three-dimensional (3D) volume rendered color-coded maps of Gd-DTPA–induced signal changes 2 h after administration of contrast into the cerebrospinal fluid (CSF) from a rat anesthetized with DEXM-I (*B*) and isoflurane (*C*). The *red* and *blue colors* represent high- and low-contrast uptake, respectively. Over the first 2 h of contrast circulation more contrast had penetrated the brain in the DEXM-I rat (*B*) when compared with isoflurane (*C*). *Scale bar*, 3 mm.

Results

Glymphatic Transport of Gd-DTPA during Isoflurane Anesthesia in Comparison with DEXM-I

Kinetic analysis of glymphatic transport has shown that not all brain regions display the same kinetic contrast profiles. Thus, for a given experimental time period (2 to 3 h), some brain regions such as the hippocampus show clear uptake and loss, although other regions are characterized by slower uptake and little or no loss.[14,21] We first assessed and compared whole-brain glymphatic transport from groups 1 and 2. During the first 40 min (from the time of Gd-DTPA delivery into CSF), whole-brain Gd-DTPA uptake was similar between the two anesthetics. However at approximately 60 min, whole-brain Gd-DTPA uptake increased with DEXM-I anesthesia compared with isoflurane, and the T1 signal peaked at approximately 19% and 12% with DEXM-I and isoflurane, respectively (fig. 1A for TSCs). The quantitative analysis of the total brain uptake of Gd-DTPA as measured by AUC_{180} (representing glymphatic transport over a 180 min CSF circulation period) demonstrated that rats anesthetized with DEXM-I had 32% higher uptake than rats anesthetized with isoflurane (AUC_{180} [brain] DEXM-I [N = 8]: 2,490 ± 446% × min *vs.* AUC_{180} [brain] isoflurane [N = 8]: 1,697 ± 431% × min; $P < 0.003$). The spatial distribution pattern of whole-brain uptake is shown as a volume-rendered color-coded map in a DEXM-I anesthetized rat (fig. 1B) and an isoflurane anesthetized rat (fig. 1C) 2 h after the start of contrast infusion, and shows more overall tissue penetration of Gd-DTPA in DEXM-I compared with isoflurane.

Figure 2A shows average scatter plots of hippocampal TSC from rats anesthetized with DEXM-I in comparison with rats anesthetized with pure isoflurane. The hippocampal TSC data can be divided into three time periods based on the kinetics: t_1 = 0 to 12.3 min presents the period of delay from the time of CSF contrast infusion into the cisterna magna until the contrast reaches the hippocampus region; t_2 = 12.3 to 61.5 min presents the period of glymphatic contrast transport where influx is greater than clearance; and t_3 = 61.5 to 160 min present the period where glymphatic contrast clearance is dominating. In the hippocampus region, the time to peak was similar between the two groups (DEXM-I [n = 8] 73.2 ± 8.7 min *vs.* isoflurane [n = 8] 63.0 ± 12.6 min; *P* value = 0.079). From the linear regression of t_3, where clearance of contrast dominated, we extracted peak magnitude and clearance rates from each rat of the two groups. The peak magnitude of contrast in DEXM-I–anesthetized rats was significantly greater compared with isoflurane-anesthetized rats (31.0 ± 9.8% *vs.* 12.6 ± 4.1%; $P = 0.0017$). In addition, the calculated clearance rate was also superior in DEXM-I–anesthetized rats compared with isoflurane: (0.12 ± 0.05%/

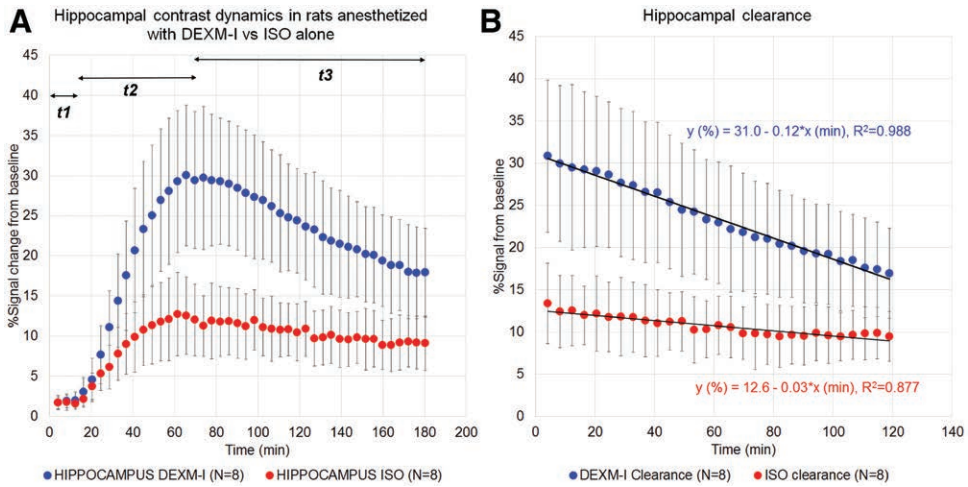

Fig. 2. Glymphatic transport in the hippocampus of rats anesthetized with dexmedetomidine plus isoflurane (DEXM-I) and isoflurane. (*A*) Average scatter plots of hippocampal time signal curves (TSC) from rats anesthetized with DEXM-I (*blue*) in comparison with rats anesthetized with pure isoflurane (*red*). The hippocampal TSC data can be divided into three time periods based on the kinetics: t_1 = 0 to 12.3 min presents the period of delay from the time of contrast infusion into the cerebrospinal fluid until the contrast reaches the hippocampus region; t_2 = 12.3 to 61.5 min presents the period of glymphatic contrast transport where influx is greater than clearance; and t_3 = 61.5 to 160 min present the period where glymphatic contrast clearance is dominating. The linear regression parameters of the average hippocampal clearance profiles from the two groups (DEXM-I, *blue*; and isoflurane, *red*) are shown in (*B*). Data are presented at mean ± SD. ISO = isoflurane.

min *vs.* 0.03 ± 0.02%/min; P = 0.0011). The linear regression parameters of the average hippocampal clearance profiles from the two groups are shown in figure 2B.

Physiologic and Cerebral Vascular Status with the Two Anesthetics

One explanation for the enhanced glymphatic transport with DEXM-I compared with isoflurane could be related to potential different actions on the cerebral vasculature. Dexmedetomidine has vasoconstrictive properties,[32] whereas isoflurane exerts intrinsic vasodilation,[33] and these differences may affect glymphatic transport. The differential effect of the two anesthetics on the cerebral vasculature and glymphatic transport are best evaluated if arterial blood pressure and respiratory status are maintained at the same level. During the MRI experiments, vital signs were recorded continuously while the rat underwent scanning. Statistical analysis revealed no differences in the RRs between the two anesthesia groups (RR [DEXM-I] = 52 ± 8 breaths/min *vs.* RR [isoflurane] = 55 ± 5 breaths/min; P = 0.37), and the RR coefficient of variability for the two groups was also similar (fig. 3). In contrast, the mean HR for rats anesthetized with DEXM-I was lower than for isoflurane (HR [DEXM-I] = 286 ± 18 beats per min *vs.* HR [isoflurane] = 342 ± 24 beats per min; P < 0.005); however, HR variability (coefficient of variation) did not differ between groups. To further evaluate physiologic profiles, we performed blood gas measurements in separate groups of rats exposed to the same two anesthetic regimes for more than 1 h during MRI scanning. These experiments confirmed similar blood gas values between the two anesthetics (Supplemental Digital Content, Table 1S, http://links.lww.com/ALN/B540).

We next explored quantitative differences in the cross-sectional large vessel diameter between the two groups based on the 2D time-of-flight MR angiograms. We measured the radial projections of four vessels, which are straightforward to locate anatomically including the superior sagittal sinus, straight sinus, external jugular vein, and internal carotid artery (ICA). Figure 4, A and B, shows typical 3D rendered MR angiograms displaying the major vascular landmarks including the vessel segments of interest highlighted in red. Isoflurane produced greater vasodilation in the straight sinus when compared with DEXM-I (compare fig. 4C with fig. 4D). In contrast, no differences in average vessel diameter were seen in the other three vessels measured (fig. 4, E and F; table 2).

Gray Matter, White Matter, and CSF Volume Effects of the Two Anesthetics

Reduced uptake of Gd-DTPA with isoflurane when compared with DEXM-I suggests that the CSF had restricted access to the glymphatic pathway of the brain. We used the quantitative T1 maps to extract the volumes of the gray matter, white matter, and CSF tissue compartments. Table 3 shows the quantitative data for total brain volume (TBV), gray matter, white matter, and CSF. As expected, there was no difference in TBV between the two groups (TBV, isoflurane = 1611 ± 117 mm^3 *vs.* TTV, DEXM-I = 1695 ± 49 mm^3). The CSF compartment was significantly decreased with isoflurane compared with DEXM-I (CSF [isoflurane] = 54 ± 8 mm^3 *vs.* CSF [DEXM-I] = 85 ± 7 mm^3; P < 0.01), supporting the statement that less CSF gains access to the brain with isoflurane.

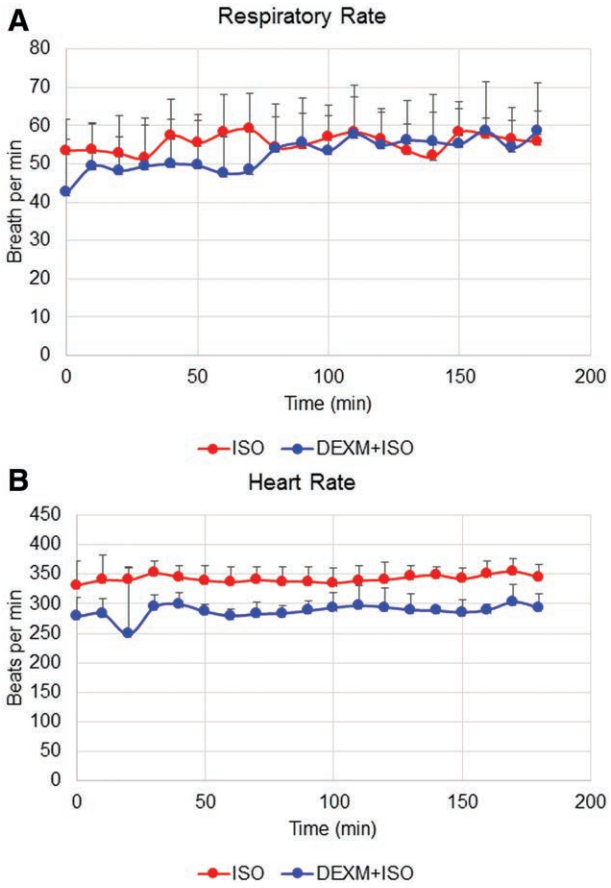

Fig. 3. Physiologic parameters during magnetic resonance imaging (MRI) scans. Respiratory rate and heart rate were recorded noninvasively during measurement of glymphatic transport with MRI. The respiratory rate for isoflurane and dexmedetomidine plus isoflurane (DEXM-I) anesthesia groups were similar over the 2- to 3-h experimental period (*A*). The heart rate was significantly lower in DEXM-I rats compared with isoflurane-anesthetized rats (*B*). The data are expressed as mean ± SD. ISO = isoflurane.

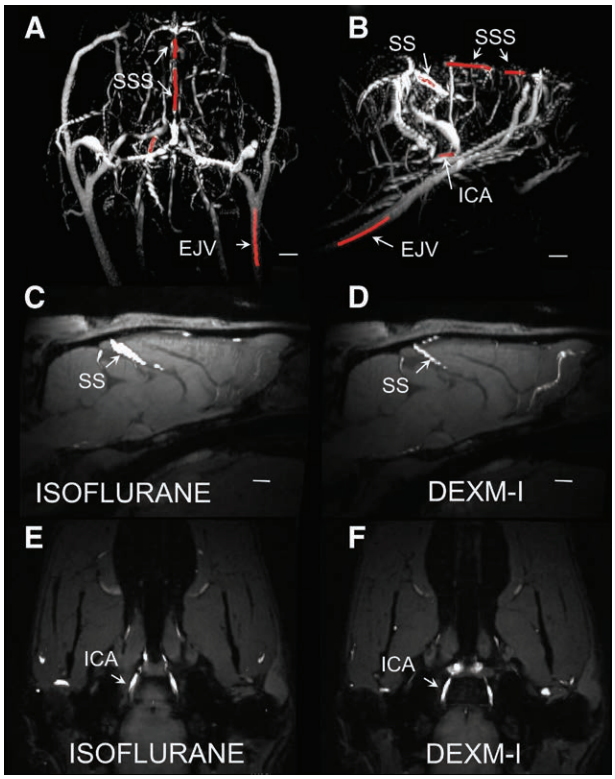

Fig. 4. Magnetic resonance (MR) angiograms from rat anesthetized with isoflurane *versus* dexmedetomidine plus isoflurane (DEXM-I). (*A* and *B*) Typical three-dimensional (3D) volume rendered MR angiograms (maximum intensity projections) displaying the major vascular landmarks including the vessel segments of interest highlighted in *red*. (*C–F*) Two-dimensional (2D) MR angiograms overlaid on the corresponding T1-weighted MR images (MRIs). Isoflurane produced greater vasodilation in the SS when compared with DEXM-I (compare *C* with *D*). In contrast, no differences in average vessel diameter were observed at the level of the ICA (compare *E* and *F*). *Scale bar*, 2 mm. ICA = internal carotid artery; EJV = external jugular vein; SS = straight sinus; SSS = superior sagittal sinus.

If CSF is not entering into the glymphatic system with isoflurane to the same extent as with DEXM-I, CSF must be diverted to other sites for reabsorption. We characterized efflux of Gd-DTPA at the olfactory portion of the nasal cavity, which is known to participate in CSF efflux.[34] The limited MRI field of view did not allow us to capture more distant areas (*e.g.*, nasoturbinates and maxilla turbinates), but the endoturbinates could be assessed. The location of the olfactory portion of the nasal cavity, which represents the innermost zone containing the endoturbinates, is shown in sagittal (fig. 5A) and cross-sectional (fig. 5B) T1-weighed MRI; note the typical spiral lamella at the level of the endoturbinates. As can be seen in figure 5C, Gd-DTPA efflux in a rat anesthetized with isoflurane (50 min after CSF administration) displays a distribution pattern similar to the outline of the endoturbinates, suggesting that it ends up in nasal submucosa similar to what has been reported in the literature.[34] Figure 5D shows the average TSCs from the nasal cavity from rats anesthetized with isoflurane *versus* DEXM-I. Both the average peak signal amplitude (51.5% *vs.* 39.0%; $P < 0.05$) and the time to peak (isoflurane, 54.3 ± 4.7 min *vs.* DEXM-I, 72.4 ± 5.6 min; $P < 0.001$) is significantly higher

Table 2. Vessel Diameter Differences between the Two Groups

Average Vessel Diameter, μm	Isoflurane (N = 8)	DEXM-I (N = 6)	*P* Value
SSS	159 ± 49	139 ± 47	0.192
SS	307 ± 73	127 ± 26	0.002
EJV	567 ± 13	448 ± 98	0.107
ICA	245 ± 59	245 ± 38	1.000

Data are presented as mean ± SD. Only six of the eight rats in the DEXM-I anesthesia group (group 2) underwent magnetic resonance angiography analysis.

DEXM-I = dexmedetomidine plus low-dose isoflurane; EJV = external jugular vein; ICA = internal carotid artery; SS = straight sinus; SSS = superior sagittal sinus.

Table 3. Total Brain Volume and Tissue Compartments between the Two Groups

	Total Brain Volume, mm^3	Grey Matter Volume, mm^3	White Matter Volume, mm^3	CSF Volume, mm^3
Isoflurane (N = 4)	1611 ± 112	924 ± 113	633 ± 41	54 ± 8
DEXM-I (N = 4)	1695 ± 49	931 ± 50	681 ± 25	84 ± 7
P value	0.210	0.602	0.076	0.009

Data are presented as mean ± SD.

CSF = cerebrospinal fluid; DEXM-I = dexmedetomidine plus isoflurane.

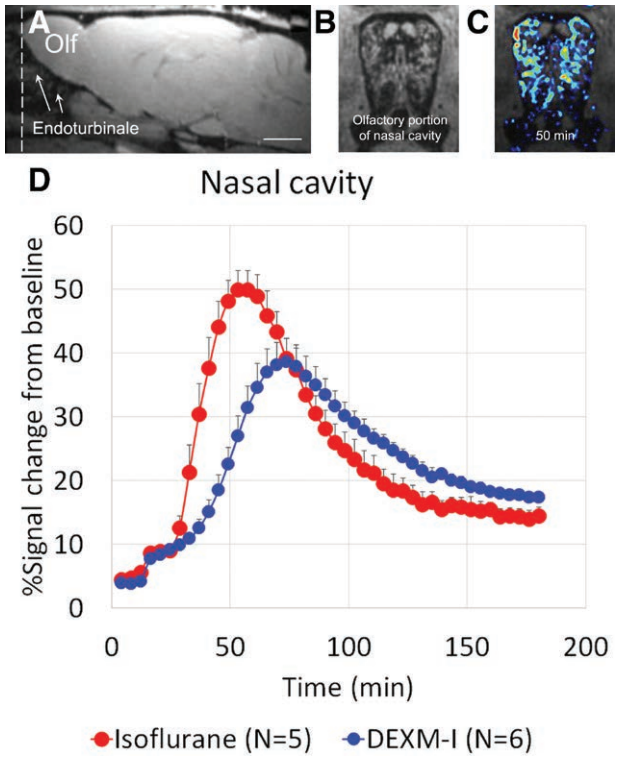

Fig. 5. Magnetic resonance (MR) contrast (gadopentetic acid [Gd-DTPA]) efflux *via* the olfactory nerves. (*A*) Sagittal T1-weighted MR imaging (MRI) at the level of the olfactory bulb and endoturbinates. The field of view includes the olfactory portion of the nasal cavity (Olf = olfactory bulb). *Scale bar*, 3 mm. The *dashed line* indicates the cross-sectional area for the nasal cavity shown in *B* (anatomy displayed) and *C* (color coded MR contrast map representing Gd-DTPA after 50 min of cerebrospinal fluid circulation overlaid on the anatomic map). As can be observed in *C*, the distribution pattern of contrast follows the surface curvature of the endoturbinates. *(D)* Average time signal curves (TSCs) acquired from the endoturbinates of rats anesthetized with isoflurane (*red*) *versus* dexmedetomidine plus isoflurane (DEXM-I, *blue*). Quantitative analysis show that the time to peak and peak amplitude of Gd-DTPA–induced signal changes are significantly higher in isoflurane compared with DEXM-I–anesthetized rats. The data are presented as mean ± SD. The data were extracted from the contrast-enhanced MRIs *via* an anatomic mask of the olfactory portion of the nasal cavity.

for isoflurane compared with DEXM-I. Together, these results suggest that, for the same time period, more CSF carrying Gd-DTPA enters into the endoturbinates with isoflurane compared with DEXM-I.

Electroencephalogram Changes with Isoflurane versus *DEXM-I*

In separate groups of rats (groups 5 and 6; table 1) electroencephalogram profiles were recorded under the two different anesthetic regimens. Figure 6 shows an example of an electroencephalogram spectrogram (2D, density spectral array; fig. 6A), an unprocessed electroencephalogram trace from a rat anesthetized with isoflurane (fig. 6B), and the corresponding electroencephalogram display in a rat anesthetized with DEXM-I (fig. 6, C and D). In the rat anesthetized with isoflurane, the 2D spectrogram representing a 7-min segment (fig. 6A) shows that, during the first 2 min, the electroencephalogram is dominated by slow delta (1 to 4 Hz) and alpha (9 to 12 Hz) oscillations followed by burst suppression. Burst suppression is described as "a state of unconsciousness and profound brain inactivation,"[18] and the raw, unprocessed electroencephalogram will often display this as alternating periods of isoelectricity and electrical activity, as shown in figure 6B. In the rats anesthetized with isoflurane, episodes of burst suppression were observed when the RR was at approximately 50 breaths/min (isoflurane approximately 1.5%). In the rats anesthetized with DEXM-I (isoflurane approximately 0.6%), spindle oscillations (9 to 15 Hz) could be observed, and examples are shown in figure 6, C and D. In the DEXM-I anesthetized rats, the spindle frequency varied, and most often the electroencephalogram was dominated by slow delta oscillations. Spindle oscillations were never observed in the rats anesthetized with isoflurane.

Discussion

In this study, we compared the effects of DEXM-I with pure isoflurane anesthesia on the glymphatic transport efficiency of the brain to address the question of whether drugs that produce unconsciousness all enhance glymphatic transport to the same extent. We hypothesized that unconsciousness produced in rodents receiving supplementary dexmedetomidine, a potent selective α2 agonist, given its blocking effect on central norepinephrine release,[17,35] would enhance glymphatic transport greater than those receiving pure isoflurane. This hypothesis was based on previous data by Xie *et al.*,[13] showing that glymphatic transport (when compared with wakefulness) was dramatically increased by xylazine/ketamine anesthesia, deep wave sleep, and α-antagonists administered directly onto the cortex. Using the MRI method developed previously[21] for quantifying glymphatic transport,

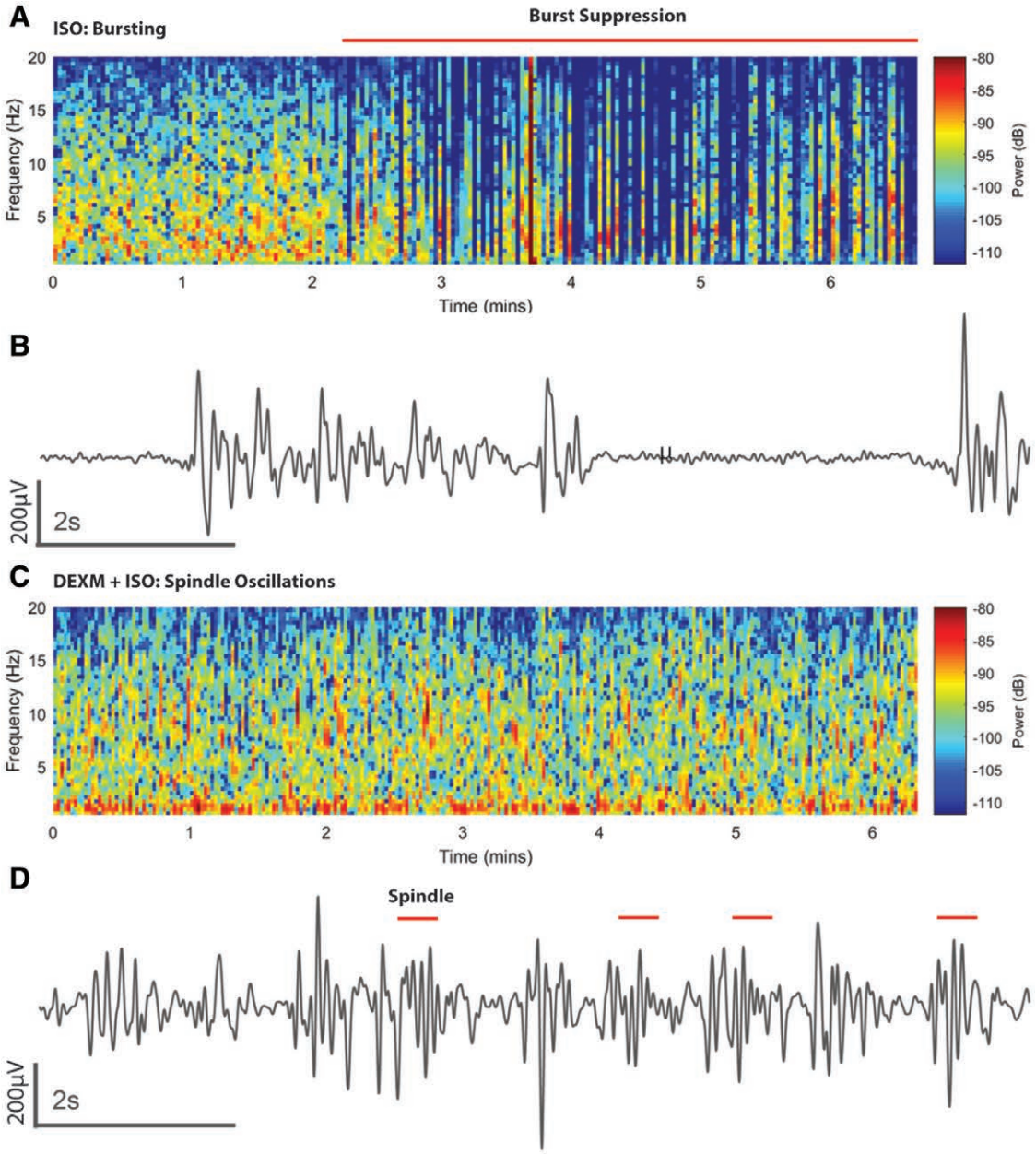

Fig. 6. Spectrograms and time domain electroencephalogram signatures of isoflurane and dexmedetomidine plus isoflurane (DEXM-I). (*A*) Two-dimensional (2D) spectrogram of electroencephalogram from a rat receiving isoflurane. Burst suppression in the spectrogram is shows as periods of *blue* (isoelectric activity) interspersed with periods of *red-yellow* (delta and theta oscillations). The *horizontal red line* shows the principal period of burst suppression. (*B*) Ten-second electroencephalogram trace from *A* showing burst events (*intermittent high amplitude activity*) and suppression events (*isoelectric activity*). (*C*) 2D electroencephalogram spectrogram from a rat receiving DEXM-I. The spectrogram shows spindles (*intermittent red period* 9 to 15 Hz) and slow-delta oscillations. (*D*) Ten-second electroencephalogram trace from the period in *C* emphasizing spindles (*red lines*). ISO = isoflurane.

we showed that glymphatic transport of the rodent brain was indeed significantly increased with DEXM-I anesthesia compared with isoflurane.

When stimulated, presynaptic α2 receptors inhibit norepinephrine release in the brain including the locus coeruleus,[17] which has the highest density of α2 receptors in the brain.[36] Locus coeruleus neurons project to the basal forebrain, preoptic area, hypothalamus, thalamus, and cortex.[18,37] The effect of norepinephrine blockade on the preoptic area, in particular, has wide-ranging upstream effects involving several neurotransmitters and neural networks, leading to decreased arousal, sleep-like states, or deep sedation.[18] In contrast, isoflurane (a halogenated inhalational anesthetic) exerts its effects by acting on a wide variety of voltage- and ligand-gated channels including γ-aminobutyric acid receptor type A, glycine, nicotinic acetylcholine receptors, *N*-methyl-D-aspartate, and

K channels,[19,38] which are located throughout the brain and spinal cord. The effects of isoflurane on locus coeruleus neurons and NE are not as clear cut as those of dexmedetomidine. Although isoflurane has been shown to depress locus coeruleus activity (this effect is most pronounced during the night cycle where locus coeruleus neurons are most active),[39] rats anesthetized with 2% isoflurane show increases in preoptic area norepinephrine.[40] Given the divergent effects of dexmedetomidine and isoflurane on norepinephrine, we expected enhanced glymphatic transport with DEXM-I anesthesia compared with isoflurane-only anesthesia. Xie *et al.*[13] administered α-antagonists directly onto the cortex of mice and observed the same increase in glymphatic transport as in deep sleep in comparison with wakefulness. Due to the experimental design, which necessitated the low-dose isoflurane with dexmedetomidine, our study cannot strictly distinguish among effects of dexmedetomidine, effects of low-dose isoflurane, or effects of the combination DEXM-I when compared with high-dose isoflurane. However, the enhanced glymphatic transport with DEXM-I compared with isoflurane is likely attributed to the potent effect of dexmedetomidine on central norepinephrine release, because the systemic sympatholytic effects were evident by a lower HR in rats receiving supplementary dexmedetomidine. In humans, intravenous DEXM infusion also reduces systemic sympathetic tone with baroreflex sensitivity preserved.[41]

The low-dose isoflurane and dexmedetomidine anesthetic regimen used in our study was shown previously to maintain blood–oxygen level–dependent functional MRI–neuronal activity coupling and was introduced specifically for rodent functional MRI brain imaging studies to demonstrate the presence of the default mode network.[42] The demonstration of a preserved default mode network with DEXM-I is strongly suggestive of a lighter state of sedation or anesthesia because the default mode network is known to be inhibited with increasing levels of anesthesia.[43] Based on this information, it is to be expected that, although the rats in our study were all unconscious during the measurement of glymphatic transport, the rats anesthetized with pure isoflurane were in a deeper state of anesthesia compared with the rats anesthetized with DEXM-I. To further investigate anesthetic depth of the two anesthetic regimens, we recorded electroencephalogram in a separate series of rats (who did not undergo MRI). In the rats receiving DEXM-I, the electroencephalogram was characterized by slow-wave oscillations and spindles, whereas the electroencephalogram with isoflurane only showed burst patterns intermingled with slow delta and alpha oscillations. These data confirm that that anesthesia with pure isoflurane produces a deeper state of anesthesia as evidenced by burst suppression compared with DEXM-I. In human subjects the electroencephalogram during dexmedetomidine sedation is characterized by slow-delta oscillations with spindles, which resemble stage II nonrapid eye movement sleep.[18] With increasing dexmedetomidine dosing and depth of sedation (unresponsive to verbal commands), the slow-delta oscillations dominate as in stage III sleep.[18] With isoflurane administered at one minimum alveolar concentration or higher, the electroencephalogram is characterized by slow delta, alpha, and theta oscillations and burst pattern. In summary, the two anesthetic drug regimens used in our experiments both produced unconsciousness (loss of righting reflex) but they had different effects on glymphatic transport, emphasizing that the underlying molecular signature of the drug producing unconsciousness is more important than anesthetic depth, *per se*.

Xie *et al.*[13] showed that when mice were asleep or anesthetized with ketamine or xylazine, the ISF space volume increased by 40 to 60% in cortex when compared with wakefulness, presumably reflecting cell volume shrinkage.[13] Accordingly, assuming that dexmedetomidine reduces central norepinephrine, the reason for enhanced glymphatic transport would suggest that ISF space volume also increases more with DEXM-I when compared with isoflurane, thereby allowing more CSF to enter the brain to exchange with ISF. In support of this statement, the quantitative analysis of tissue compartments based on T1 maps revealed that the CSF compartment was significantly larger (approximately 2%) in DEXM-I–anesthetized rats compared with isoflurane only. This result suggests that more CSF enters the glymphatic pathway in the rats anesthetized with DEXM-I, thereby enhancing convective solute exchange and transport. It is important to point out that we only measured CSF volume and not CSF production. Other studies have shown that isoflurane anesthesia does not appear to affect CSF production[44] but may affect reabsorption. The possibility that isoflurane may affect CSF reabsorption patterns is supported by evidence of enhanced egress of Gd-DTPA *via* the olfactory nerves in isoflurane-anesthetized rats when compared with DEXM-I (fig. 5).

The RRs of the rats in the two anesthesia groups were similar during the MRI experiments, and it is unlikely therefore that hypercarbia, secondary vasodilation, and increased ICP are explanatory factors for the observed differences in the glymphatic transport. This statement is supported by data from a separate group of rats demonstrating similar arterial blood gases with the two anesthetics. Future experiments quantifying ICP would be required to rule out this possibility. However, inhalational anesthetics including isoflurane are known to have intrinsic vasodilatory effects. Indeed, the MR angiograms did suggest that certain vascular beds, such as the straight sinus, were more dilated with isoflurane compared with DEXM-I (fig. 4). Because the straight sinus is situated near the pineal recess, which is a large CSF reservoir in the rat brain, extreme straight sinus dilatation with isoflurane anesthesia might also explain the observed reduced influx of CSF. Additional improvement in quantitative MR angiogram analysis and supplementary quantitative measurement of cerebral blood volume and cerebral blood flow (CBF) will be needed to more fully address the impact of divergent vascular beds on glymphatic transport with the two anesthetics. However, previous rodent studies have

shown that isoflurane anesthesia delivered at 1.7% results in an approximately 50% increase in CBF and approximately 10% increase in cerebral blood volume in comparison with propofol.[45] It is also known that sedation with low-dose dexmedetomidine decreases CBF up to 30% in healthy volunteers,[32] and it has been suggested that this effect is in part due to stimulation of α_{2B}-receptors by dexmedetomidine producing vasoconstriction. However, we did not observe vasoconstriction at the level of the internal carotid artery in the DEXM-I–anesthetized rats when compared with isoflurane, which could be due to the low dose of isoflurane used and/or limitation in our techniques.

Limitations of the Study

The MRI-based platform for quantifying glymphatic transport in the rodent brain has been validated using optical imaging and fluorescently tagged dyes administered into CSF.[1,14,21] Thus, both periarterial influx and parenchymal uptake of the MR contrast agent have been shown to mimic periarterial and parenchymal transport of small molecular weight fluorescently tagged dyes.[21] From these studies a quantitative measure of glymphatic transport and clearance have been derived. However, it has to be pointed out that brain parenchymal clearance of the extracellular, metabolically inert solute Gd-DTPA is a net effect of redistribution and elimination, and thus it is possible that the enhanced clearance observed in DEXM-I–anesthetized rats compared with isoflurane reflects faster redistribution rather than true clearance. Additional investigations with other solutes and quantitative tools will help determine these parameters more accurately.

Potential Clinical Implications

The glymphatic pathway of the brain has received tremendous research attention because of its role in removal of metabolic wastes, including soluble Aβ and tau,[1,2] and the therapeutic potential of manipulating this pathway for preventing or slowing down AD.[46] In addition, the notion that sleep enhances Aβ clearance *via* the glymphatic pathway and the fact that chronic sleep disorders are associated with a higher risk for development of AD[47] suggest that potentially simple preventive clinical measures such as facilitating better overall quality of sleep might help reduce the risk of AD. Although not yet demonstrated, there are data in support of a human glymphatic pathway including the following: (1) circadian variation in the CSF concentration of Aβ and tau[48]; (2) larger Aβ burden in older adults who are reporting poorer sleep quality[49]; and (3) a significant loss of aquaporin 4 expression in postmortem human brains afflicted with AD.[10] Thus, assuming that a glymphatic pathway exists in the human brain, several implications for clinical care undoubtedly will emerge in the near future.

In this study we show that, compared with isoflurane, DEXM-I enhances glymphatic transport and increases CSF volume in the rodent brain. This is important because dexmedetomidine is known to reduce other anesthetic agent requirements and is used as an adjunct in many clinical settings for sedation and/or anesthesia. Thus, it is possible that it would be advantageous to use dexmedetomidine with the goal of improving postoperative cognitive performance by improving brain waste removal during anesthesia and/or sedation procedures. In support of this conjecture, increasing clinical evidence is emerging that dexmedetomidine may prevent delirium in elderly patients after surgery,[50,51] whereas a recent study showed that a prophylactic low-dose infusion of dexmedetomidine in patients admitted to the intensive care unit after noncardiac surgery decreased the incidence of delirium in the first seven days.[52]

Acknowledgments

The authors greatly acknowledge the assistance of Mei Yu, B.S., Department of Anesthesiology, Stony Brook Medicine (Stony Brook, New York), for technical help with the animal magnetic resonance imaging experiments.

Research Support

Supported by grant Nos. R01AG048769 and RF1 AG053991 from the National Institutes of Health (Bethesda, Maryland), National Institute on Drug Abuse Intramural Research Program (Baltimore, Maryland), and Fondation Leducq (Paris, France).

Competing Interests

The authors declare no competing interests.

Correspondence

Address correspondence to Dr. Benveniste: Department of Anesthesiology, Yale School of Medicine, 333 Cedar Street, TMP3, Rm. 339, New Haven, Connecticut 06520-8089. helene.benveniste@yale.edu. Information on purchasing reprints may be found at www.anesthesiology.org or on the masthead page at the beginning of this issue. ANESTHESIOLOGY's articles are made freely accessible to all readers, for personal use only, 6 months from the cover date of the issue.

References

1. Iliff JJ, Wang M, Liao Y, Plogg BA, Peng W, Gundersen GA, Benveniste H, Vates GE, Deane R, Goldman SA, Nagelhus EA, Nedergaard M: A paravascular pathway facilitates CSF flow through the brain parenchyma and the clearance of interstitial solutes, including amyloid β. Sci Transl Med 2012; 4:147ra111
2. Iliff JJ, Chen MJ, Plog BA, Zeppenfeld DM, Soltero M, Yang L, Singh I, Deane R, Nedergaard M: Impairment of glymphatic pathway function promotes tau pathology after traumatic brain injury. J Neurosci 2014; 34:16180–93
3. Lundgaard I, Lu ML, Yang E, Peng W, Mestre H, Hitomi E, Deane R, Nedergaard M: Glymphatic clearance controls state-dependent changes in brain lactate concentration. J Cereb Blood Flow Metab 2017; 37:2112–24
4. Peng W, Achariyar TM, Li B, Liao Y, Mestre H, Hitomi E, Regan S, Kasper T, Peng S, Ding F, Benveniste H, Nedergaard M, Deane R: Suppression of glymphatic fluid transport in a mouse model of Alzheimer's disease. Neurobiol Dis 2016; 93:215–25
5. Bechter K, Hof PR, Benveniste H: On the flow dynamics of cerebrospinal fluid. Neurol Psychiatry Brain Res. 2015; 21: 96–103

6. Cserr HF, Cooper DN, Suri PK, Patlak CS: Efflux of radiolabeled polyethylene glycols and albumin from rat brain. Am J Physiol 1981; 240:F319–28
7. Louveau A, Smirnov I, Keyes TJ, Eccles JD, Rouhani SJ, Peske JD, Derecki NC, Castle D, Mandell JW, Lee KS, Harris TH, Kipnis J: Structural and functional features of central nervous system lymphatic vessels. Nature 2015; 523:337–41
8. Zakharov A, Papaiconomou C, Djenic J, Midha R, Johnston M: Lymphatic cerebrospinal fluid absorption pathways in neonatal sheep revealed by subarachnoid injection of Microfil. Neuropathol Appl Neurobiol 2003; 29:563–73
9. Kress BT, Iliff JJ, Xia M, Wang M, Wei HS, Zeppenfeld D, Xie L, Kang H, Xu Q, Liew JA, Plog BA, Ding F, Deane R, Nedergaard M: Impairment of paravascular clearance pathways in the aging brain. Ann Neurol 2014; 76:845–61
10. Zeppenfeld DM, Simon M, Haswell JD, D'Abreo D, Murchison C, Quinn JF, Grafe MR, Woltjer RL, Kaye J, Iliff JJ: Association of perivascular localization of aquaporin-4 with cognition and Alzheimer disease in aging brains. JAMA Neurol 2017; 74:91–9
11. Sakka L, Coll G, Chazal J: Anatomy and physiology of cerebrospinal fluid. Eur Ann Otorhinolaryngol Head Neck Dis 2011; 128:309–16
12. Iliff JJ, Wang M, Zeppenfeld DM, Venkataraman A, Plog BA, Liao Y, Deane R, Nedergaard M: Cerebral arterial pulsation drives paravascular CSF-interstitial fluid exchange in the murine brain. J Neurosci 2013; 33:18190–9
13. Xie L, Kang H, Xu Q, Chen MJ, Liao Y, Thiyagarajan M, O'Donnell J, Christensen DJ, Nicholson C, Iliff JJ, Takano T, Deane R, Nedergaard M: Sleep drives metabolite clearance from the adult brain. Science 2013; 342:373–7
14. Lee H, Xie L, Yu M, Kang H, Feng T, Deane R, Logan J, Nedergaard M, Benveniste H: The effect of body posture on brain glymphatic transport. J Neurosci 2015; 35:11034–44
15. Ding F, O'Donnell J, Xu Q, Kang N, Goldman N, Nedergaard M: Changes in the composition of brain interstitial ions control the sleep-wake cycle. Science 2016; 352:550–5
16. Keating GM, Hoy SM, Lyseng-Williamson KA: Dexmedetomidine: A guide to its use for sedation in the US. Clin Drug Investig 2012; 32:561–7
17. Jorm CM, Stamford JA: Actions of the hypnotic anaesthetic, dexmedetomidine, on noradrenaline release and cell firing in rat locus coeruleus slices. Br J Anaesth 1993; 71:447–9
18. Purdon PL, Sampson A, Pavone KJ, Brown EN: Clinical electroencephalography for anesthesiologists: Part I–Background and basic signatures. Anesthesiology 2015; 123:937–60
19. Mashour GA, Forman SA, Campagna JA: Mechanisms of general anesthesia: From molecules to mind. Best Pract Res Clin Anaesthesiol 2005; 19:349–64
20. Kushikata T, Hirota K, Kotani N, Yoshida H, Kudo M, Matsuki A: Isoflurane increases norepinephrine release in the rat preoptic area and the posterior hypothalamus *in vivo* and *in vitro*: Relevance to thermoregulation during anesthesia. Neuroscience 2005; 131:79–86
21. Iliff JJ, Lee H, Yu M, Feng T, Logan J, Nedergaard M, Benveniste H: Brain-wide pathway for waste clearance captured by contrast-enhanced MRI. J Clin Invest 2013; 123:1299–309
22. Stollberger R, Wach P: Imaging of the active B1 field *in vivo*. Magn Reson Med 1996; 35:246–51
23. Frahm J: Rapid FLASH NMR imaging. Naturwissenschaften 1987; 74:415–22
24. Chang LC, Koay CG, Basser PJ, Pierpaoli C: Linear least-squares method for unbiased estimation of T1 from SPGR signals. Magn Reson Med 2008; 60:496–501
25. Cheng HL, Wright GA: Rapid high-resolution T(1) mapping by variable flip angles: accurate and precise measurements in the presence of radiofrequency field inhomogeneity. Magn Reson Med 2006; 55:566–74
26. Deoni SC, Peters TM, Rutt BK: Determination of optimal angles for variable nutation proton magnetic spin-lattice, T1, and spin-spin, T2, relaxation times measurement. Magn Reson Med 2004; 51:194–9
27. Ashburner J, Friston KJ: Unified segmentation. Neuroimage 2005; 26:839–51
28. Valdés-Hernández PA, Sumiyoshi A, Nonaka H, Haga R, Aubert-Vásquez E, Ogawa T, Iturria-Medina Y, Riera JJ, Kawashima R: An *in vivo* MRI template set for morphometry, tissue segmentation, and fMRI localization in rats. Front Neuroinform 2011; 5:26
29. Lee H, Mortensen K, Sanggaard S, Koch P, Brunner H, Quistorff B, Nedergaard M, Benveniste H: Quantitative Gd-DOTA uptake from cerebrospinal fluid into rat brain using 3D VFA-SPGR at 9.4T. Magn Reson Med 2017 Jun 19 [Epub ahead of print]
30. Li Y, Shen Q, Huang S, Li W, Muir ER, Long JA, Duong TQ: Cerebral angiography, blood flow and vascular reactivity in progressive hypertension. Neuroimage 2015; 111:329–37
31. Veasey SC, Valladares O, Fenik P, Kapfhamer D, Sanford L, Benington J, Bucan M: An automated system for recording and analysis of sleep in mice. Sleep 2000; 23:1025–40
32. Prielipp RC, Wall MH, Tobin JR, Groban L, Cannon MA, Fahey FH, Gage HD, Stump DA, James RL, Bennett J, Butterworth J: Dexmedetomidine-induced sedation in volunteers decreases regional and global cerebral blood flow. Anesth Analg 2002; 95:1052–9
33. Matta BF, Heath KJ, Tipping K, Summors AC: Direct cerebral vasodilatory effects of sevoflurane and isoflurane. Anesthesiology 1999; 91:677–80
34. Johnston M, Zakharov A, Koh L, Armstrong D: Subarachnoid injection of Microfil reveals connections between cerebrospinal fluid and nasal lymphatics in the non-human primate. Neuropathol Appl Neurobiol 2005; 31:632–40
35. Callado LF, Stamford JA: Alpha2A- but not alpha2B/C-adrenoceptors modulate noradrenaline release in rat locus coeruleus: Voltammetric data. Eur J Pharmacol 1999; 366:35–9
36. Zilles K, Qü M, Schleicher A: Regional distribution and heterogeneity of alpha-adrenoceptors in the rat and human central nervous system. J Hirnforsch 1993; 34:123–32
37. Akeju O, Loggia ML, Catana C, Pavone KJ, Vazquez R, Rhee J, Contreras Ramirez V, Chonde DB, Izquierdo-Garcia D, Arabasz G, Hsu S, Habeeb K, Hooker JM, Napadow V, Brown EN, Purdon PL: Disruption of thalamic functional connectivity is a neural correlate of dexmedetomidine-induced unconsciousness. Elife 2014; 3:e04499
38. Pal D, Silverstein BH, Lee H, Mashour GA: Neural correlates of wakefulness, sleep, and general anesthesia: An experimental study in rat. Anesthesiology 2016; 125:929–42
39. Gompf H, Chen J, Sun Y, Yanagisawa M, Aston-Jones G, Kelz MB: Halothane-induced hypnosis is not accompanied by inactivation of orexinergic output in rodents. Anesthesiology 2009; 111:1001–9
40. Anzawa N, Kushikata T, Ohkawa H, Yoshida H, Kubota T, Matsuki A: Increased noradrenaline release from rat preoptic area during and after sevoflurane and isoflurane anesthesia. Can J Anaesth 2001; 48:462–5
41. Hogue CW Jr, Talke P, Stein PK, Richardson C, Domitrovich PP, Sessler DI: Autonomic nervous system responses during sedative infusions of dexmedetomidine. Anesthesiology 2002; 97:592–8
42. Lu H, Zou Q, Gu H, Raichle ME, Stein EA, Yang Y: Rat brains also have a default mode network. Proc Natl Acad Sci USA 2012; 109:3979–84
43. Guldenmund P, Demertzi A, Boveroux P, Boly M, Vanhaudenhuyse A, Bruno MA, Gosseries O, Noirhomme Q, Brichant JF, Bonhomme V, Laureys S, Soddu A: Thalamus, brainstem and salience network connectivity changes during propofol-induced sedation and unconsciousness. Brain Connect 2013; 3:273–85

44. Abas M, Vanderpyl J, Le Prou T, Kydd R, Emery B, Foliaki SA: Psychiatric hospitalization: Reasons for admission and alternatives to admission in South Auckland, New Zealand. Aust N Z J Psychiatry 2003; 37:620–5
45. Todd MM, Weeks J: Comparative effects of propofol, pentobarbital, and isoflurane on cerebral blood flow and blood volume. J Neurosurg Anesthesiol 1996; 8:296–303
46. Nedergaard M: Neuroscience: Garbage truck of the brain. Science 2013; 340:1529–30
47. Ooms S, Overeem S, Besse K, Rikkert MO, Verbeek M, Claassen JA: Effect of 1 night of total sleep deprivation on cerebrospinal fluid β-amyloid 42 in healthy middle-aged men: A randomized clinical trial. JAMA Neurol 2014; 71:971–7
48. Roh JH, Jiang H, Finn MB, Stewart FR, Mahan TE, Cirrito JR, Heda A, Snider BJ, Li M, Yanagisawa M, de Lecea L, Holtzman DM: Potential role of orexin and sleep modulation in the pathogenesis of Alzheimer's disease. J Exp Med 2014; 211:2487–96
49. Spira AP, Gamaldo AA, An Y, Wu MN, Simonsick EM, Bilgel M, Zhou Y, Wong DF, Ferrucci L, Resnick SM: Self-reported sleep and β-amyloid deposition in community-dwelling older adults. JAMA Neurol 2013; 70:1537–43
50. Brown EN, Purdon PL, Van Dort CJ: General anesthesia and altered states of arousal: A systems neuroscience analysis. Annu Rev Neurosci 2011; 34:601–28
51. Jansson CC, Pohjanoksa K, Lang J, Wurster S, Savola JM, Scheinin M: Alpha2-adrenoceptor agonists stimulate high-affinity GTPase activity in a receptor subtype-selective manner. Eur J Pharmacol 1999; 374:137–46
52. Vemparala S, Domene C, Klein ML: Computational studies on the interactions of inhalational anesthetics with proteins. Acc Chem Res 2010; 43:103–10

ANESTHESIOLOGY REFLECTIONS FROM THE WOOD LIBRARY-MUSEUM

From Brooklyn's Master Laughing Gasser: "Dr. Colton's Dentifrice… for Rigg's Disease"

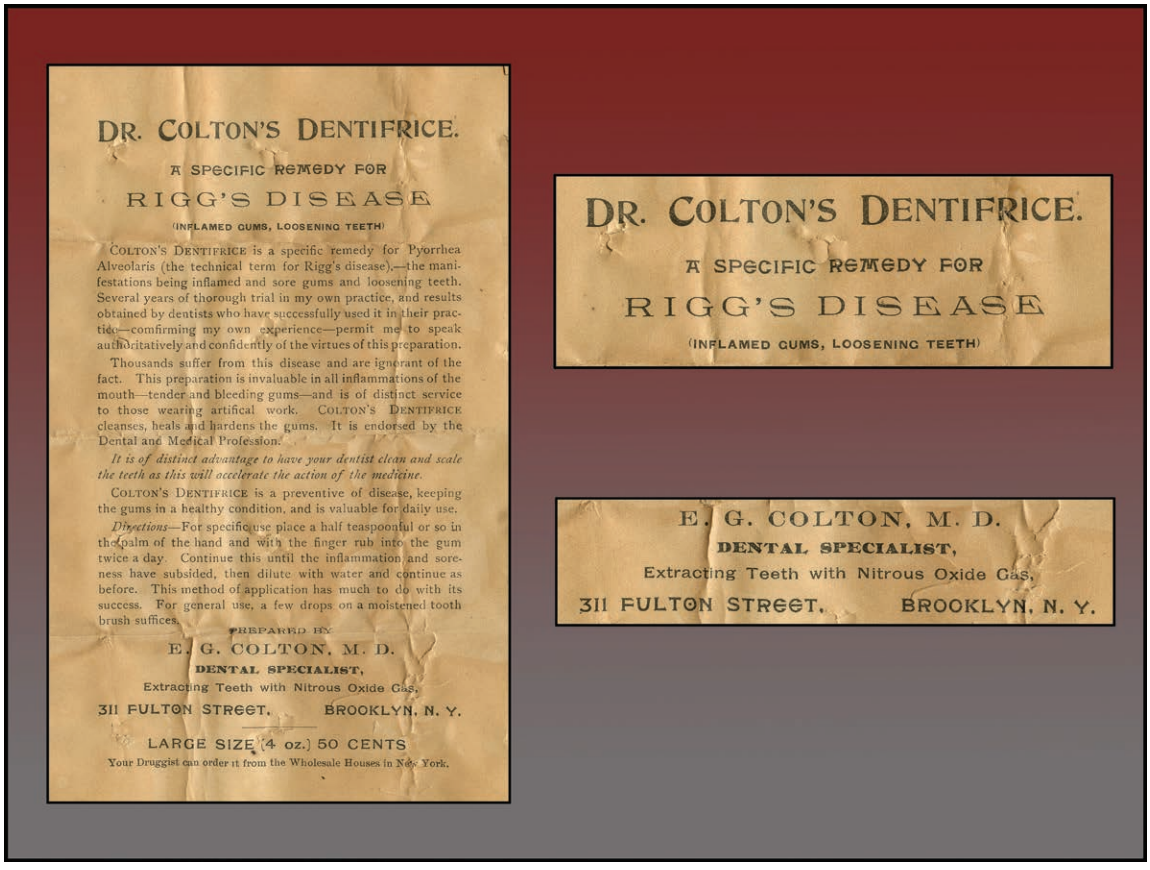

In 1844 Gardner Q. Colton administered nitrous oxide while dentist John M. Riggs (1811 to 1885) extracted a molar from his volunteer patient, nitrous-oxide pioneer Dr. Horace Wells. Dr. Riggs would be honored eventually by the dental eponym "Rigg's disease"; Colton, by his namesake Manhattan firm, the Colton Dental Association (CDA), which provided nitrous oxide for dental anesthesia. When Colton franchised his CDA to Brooklyn, New York, he placed in charge his nephew Edward Gould Colton, M.D. (1841 to 1930). An 1868 graduate of the Bellevue Hospital Medical College, E. G. Colton practiced and lived in Brooklyn for more than 60 yr. Swinging full circle, Dr. E. G. Colton would peddle his own answer (*above*) to the malady named after Riggs, the first dentist for whom "Uncle Gardner" Colton furnished nitrous oxide. On this 1910s advertisement from the Wood Library-Museum's Ben Z. Swanson Collection, E. G. Colton, M.D., advertised his own proprietary "Dr. Colton's Dentifrice" as "A Specific Remedy for Rigg's Disease (Inflamed Gums, Loosening Teeth)." (Copyright © the American Society of Anesthesiologists' Wood Library-Museum of Anesthesiology.)

George S. Bause, M.D., M.P.H., Honorary Curator and Laureate of the History of Anesthesia, Wood Library-Museum of Anesthesiology, Schaumburg, Illinois, and Clinical Associate Professor, Case Western Reserve University, Cleveland, Ohio. UJYC@aol.com.